In the case of GA and GP additional complications are introduced due to their ionic nature. As is seen in *Figure 3* the positively charged GA is less retarded than NAG while the divalent anion GP shows the strongest concentration dependence. This might partly be attributed to different hydration of the solutes, since the number of potential sites for hydrogen bonding is larger in GP than in GA, thus resulting in differences in the effective volume of the diffusing species. It is clear that the diffusion of small molecules in polymer systems is a complex phenomenon dependent on the nature of both diffusant and polymer matrix.

Acknowledgements

We thank R. Bergman for technical advice in performing the measurements.

References

1 Wang, J. H., Anfinsen, C. B. and Poleska, M. *J. Am. Chem. Soc.* 1954, **76**, 4763
2 Biancheria, A. and Kegeles, G. *J. Am. Chem. Soc.* 1957, **79**, 5908
3 Li, S. U. and Gainer, J. L. *Ind. Chem. Fundam.* 1968, **7**, 433
4 Powell, F. E. *J. Colloid Interface Sci.* 1971, **35**, 152
5 Osmers, H. R. and Metzner, A. B. *Ind. Eng. Chem. Fundam.* 1972, **11**, 161
6 Kitchen, G., *Thesis*, Monash University, Clayton, Victoria, Australia, 1975
7 Brown, W., Kloow, G., Chitumbo, K. and Amu, T. *J. Chem. Soc. Faraday Trans. I* 1976, **72**, 485
8 Namikawa, R., Okazaki, P., Nakamishi, K., Matsuno, R. and Kamikubo, T. *Agric. Biol. Chem.* 1977, **41**, 1003
9 Iijima, T., Uemura, T., Tsuzuku, S. and Komiyama, J. *J. Polym. Sci., Polym. Phys. Edn.* 1978, **16**, 793
10 Nyström, B. and Roots, J. *Eur. Polym. J.* 1980, **16**, 201
11 Moseley, M. E. and Stilbs, P. *Chem. Scripta* 1980, **16**, 114
12 Roots, J. Moseley, M. E. and Nyström, B. *Chem. Scripta* 1980, **16**, 201
13 Nyström, B., Moseley, M. E., Stilbs, P. and Roots, J. *Polymer* 1981, **22**, 218
14 Wang, J. H. *J. Am. Chem. Soc.* 1954, **76**, 4755
15 Mackie, J. S. and Meares, P. *Proc. Roy. Soc. Lond.* 1955, **A232**, 498
16 Prager, S. *J. Chem. Phys.* 1960, **33**, 122
17 Bergman, R. and Sunderlöf, L.-O. *Eur. Polym. J.* 1977, **13**, 881
18 Sundelöf, L.-O. *Arkiv Kemi* 1966, **25**, 1
19 Neurath, H. *Science* 1941, **93**, 431
20 Nernst, W. *Z. Phys. Chem.* 1888, **2**, 613

The irreversibility of dimensional changes in epoxy adhesives undergoing uptake and expulsion of water

J. P. Sargent and K. H. G. Ashbee
University of Bristol, H. H. Wills Physics Laboratory, Royal Fort, Tyndall Avenue, Bristol, England BS8 1TL, UK
(*Received* 28 *September* 1981; *revised* 17 *November* 1981)

An optical interference method, developed to measure swelling inhomogeneities during water uptake by epoxy-based adhesive films[1], has now been used to study the extent of dimensional recovery during subsequent removal of the water responsible for swelling. A microscope cover slip is employed as marker to evaluate displacements normal to a resin film that is sandwiched between it and a rigid substrate. By placing an optical flat close to the free surface of the cover slip, a cavity is created within which optical interference can occur between light incident upon and light reflected from the specimen. Normal displacements in the resin cause similar displacements in the cover slip, i.e. the geometry of the cavity is altered, and this produces changes in the pattern of interference fringes. It is found that repeated exposure of the specimen to both wet and dry environments (distilled water at 62°C and dry air at 62°C) leads to reversible changes in the displacement field normal to the adhesive film when the exposure is relatively modest (~1 day at 62°C), but that prolonged exposure (>2 days at 62°C) produces irreversible changes.

Keywords Adhesives; water-uptake; swelling; irreversibility; interferometry; Moiré-images

Introduction

Indirect experiments suggest that the accommodation of water by epoxy resins and the consequences of this accommodation are reversible. Thus, the increase in weight during water uptake can be more or less reversed by drying. So too can the associated change in glass transition temperature[2]. The information sought by the experiments reported here relates to the dimensional stability of resins during the uptake and expulsion of diffused water and is, therefore, more fundamental to an understanding of the apparent reversibility of accommodation of water.

Experimental

Method. Adhesive joints consisting of a 19 mm diameter, 0.15 mm thick microscope cover slip, are bonded with an adhesive film to a rigid substrate. These are mounted inside a controlled humidity chamber so that the free surface of the cover slip is in close proximity to an optical flat. The gap between cover slip and optical flat is made small enough to cause interference between incident and reflected light, and changes in the pattern of interference are photographed during the swelling and shrinking of the adhesive film that accompany water uptake and expulsion respectively.

In order to obtain the normal displacement field, photographs of the interference pattern taken during a run are superimposed on to a 'base line' photograph of the same interference pattern, but taken at the start of the run, so as to generate a system of Moiré fringes which bear a 1:1 correlation to the cover slip deformation.

Full details of the experimental method have been published by Sargent and Ashbee[1].

Results

Figure 1(a) is a sequence of Moiré images obtained for a specimen manufactured from American Cyanamid FM

0032-3861/82/030327-05$03.00
©1982 Butterworth & Co (Publishers) Ltd.

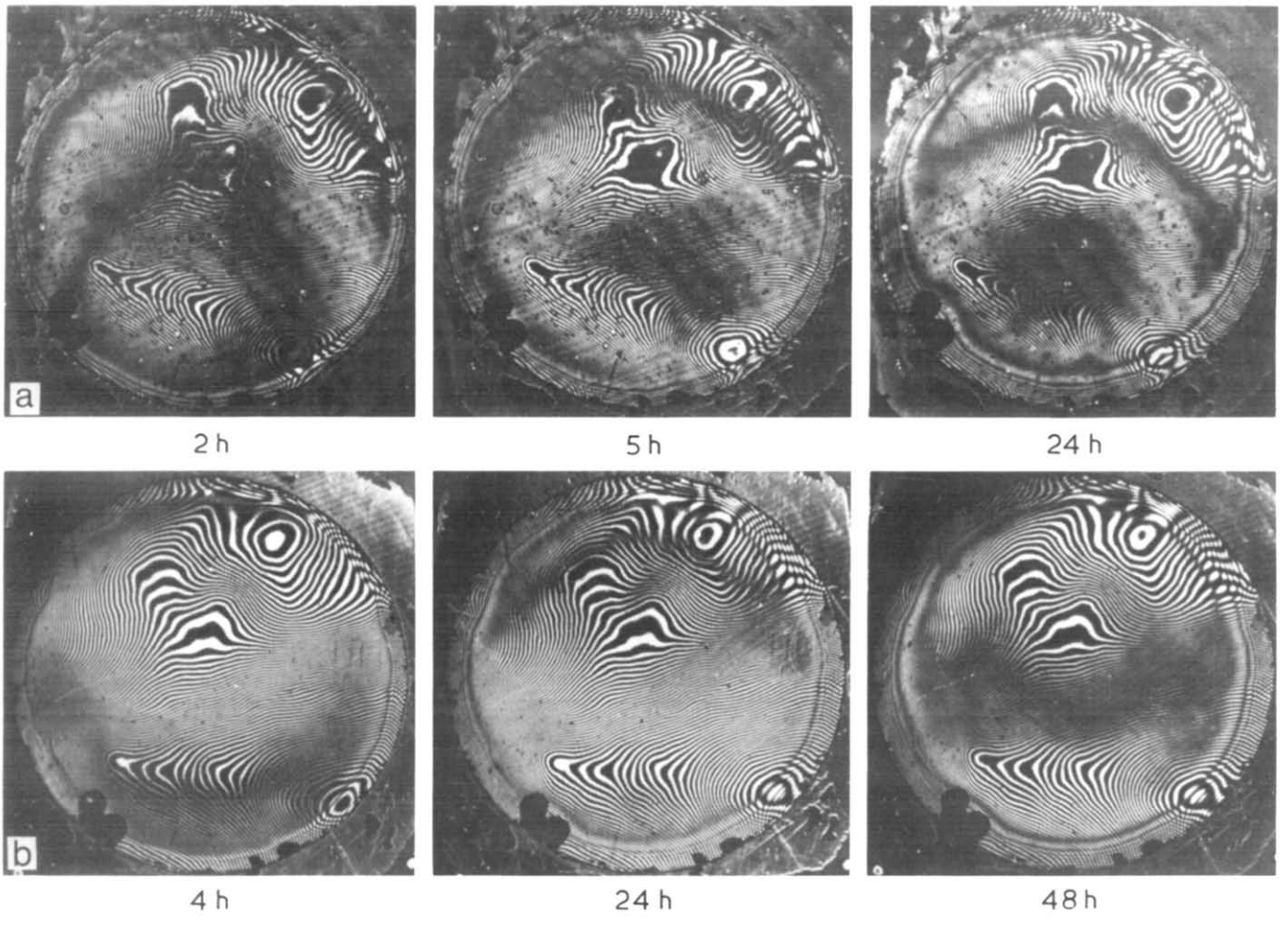

Figure 1 (a) Part of a sequence of Moiré images taken during the 62°C water uptake experiment. (b) Part of a sequence of Moiré images taken during subsequent expulsion of the water absorbed in (a)

73M and formed by superimposition on to the photograph taken at time $t=0$, corresponding to the commencement of water uptake. *Figure 1(b)* is another sequence taken during subsequent expulsion of this water; drying was also carried out at 62°C and the 'base line' photograph for the drying sequence was that taken at $t=1$ day, i.e. that corresponding to the commencement of water expulsion. Adjacent Moiré fringes in *Figures 1(a)* and *(b)* are the loci of points which differ by half a wavelength in their displacement normal to the plane of the joint. Thus, the innermost Moiré fringe in each photograph is displaced relative to the centre of the joint by a distance $w=\lambda/2\mu$ where $\lambda=546.1$ nm is the wavelength of the mercury vapour light used to illuminate the joint. $\mu=1.33$ is the refractive index of distilled water. The second from innermost fringe is displaced relative to the centre by distance $w=2\lambda/2\mu$ etc.

Figure 2 is a plot of the % displacement of a point immediately adjacent to the edge of the specimen over several cycles of water uptake and expulsion.

Creation of Moiré patterns from images photographed at identical amounts of swelling, and which are separated by one or more water uptake/expulsion cycles, permits immediate detection of any irreversible changes in the adhesive film dimensions. *Figure 3(a)* is a Moiré pattern formed between photographs taken at the points referred to as A and A′ in *Figure 2* (representing states of maximum water uptake). *Figure 3(b)* is another pattern corresponding to B and B′ in *Figure 2* (representing states of minimum water uptake). Although the absence of any circumferential Moiré patterns in either of the *Figures 3(a)* or *3(b)* indicates that repeated cycling has so far not led to any substantial irreversible changes in the displacement fields, small changes are evident. One such change is indicated by an arrow in *Figure 3(b)* and shows the appearance of small Moiré loop indicating that a permanent irreversible local swelling displacement has occurred.

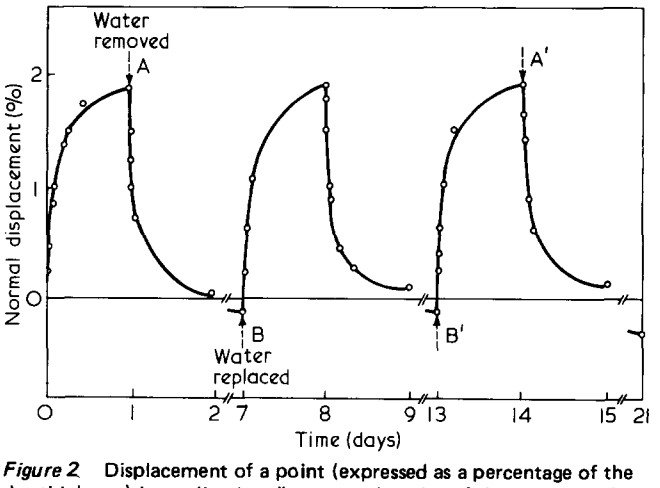

Figure 2 Displacement of a point (expressed as a percentage of the dry thickness) immediately adjacent to the edge of the specimen during several cycles of water uptake and expulsion

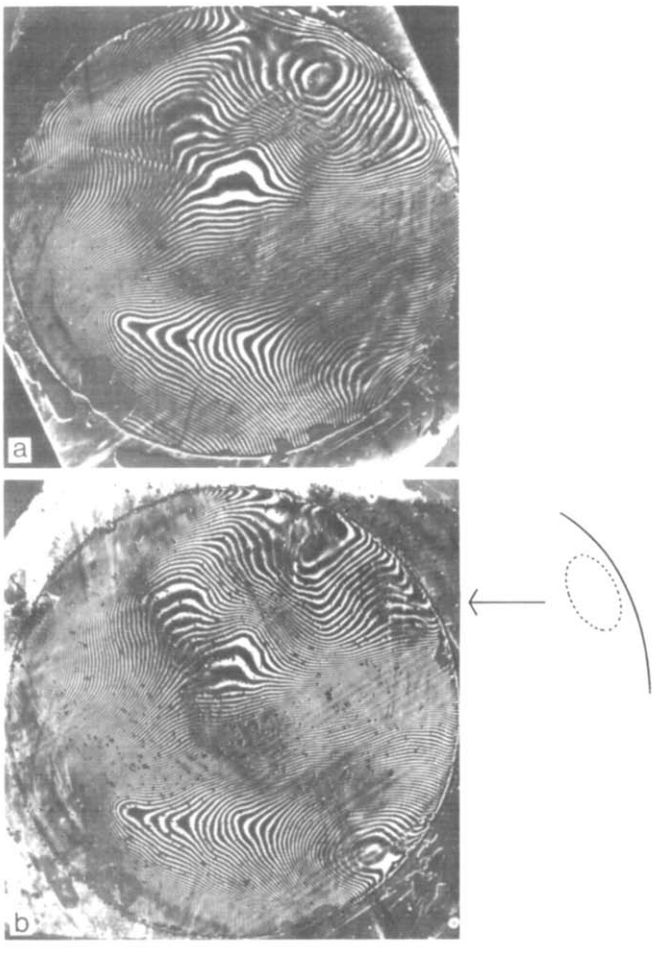

Figure 3 (a) Moiré image formed between photographs taken at points indicated as A and A′ in *Figure 2*. (b) Moiré image formed between photographs taken at points indicated as B and B′ in *Figure 2*

In order to investigate specimen behaviour when subjected to longer immersion periods a second specimen was prepared. *Figure 4*(*a*) and (*b*) are sequences of interference photographs taken during 62°C water uptake and expulsion respectively. It is evident that the cover slip began to debond after about 48 h into the water uptake half of the cycle. Debonded areas are distinguished from bonded areas by their lighter appearance; this is due to a change in the reflection coefficient at the cover slip/adhesive layer interface. When water collects at the interface, there is an increase in the refractive index mismatch and this causes a larger proportion of the incident light to be reflected back into the camera. The initiation of debonding is indicated by an arrow in the 2nd photograph in *Figure 4*(*a*). Substantial debonded areas were evident after 240 h immersion. Formation of a Moiré image between photographs of the specimen at time $t = 0$ and at the end of the drying half cycle ($t = 720$ h) reveal a complex net residual displacement in those regions where debonding has occurred.

The edge of the debonded area is relatively ill-defined in *Figure 4*. *Figure 5* is a sequence of interference patterns in which the debonding area has a well defined edge. This specimen was made using Cyanamid FM 1000

Figure 4 Sequence of interference photographs for a second FM 73M specimen, (a) immersed in distilled water at 62°C and (b) exposed to dry air at 62°C. The arrow indicates the onset of debonding

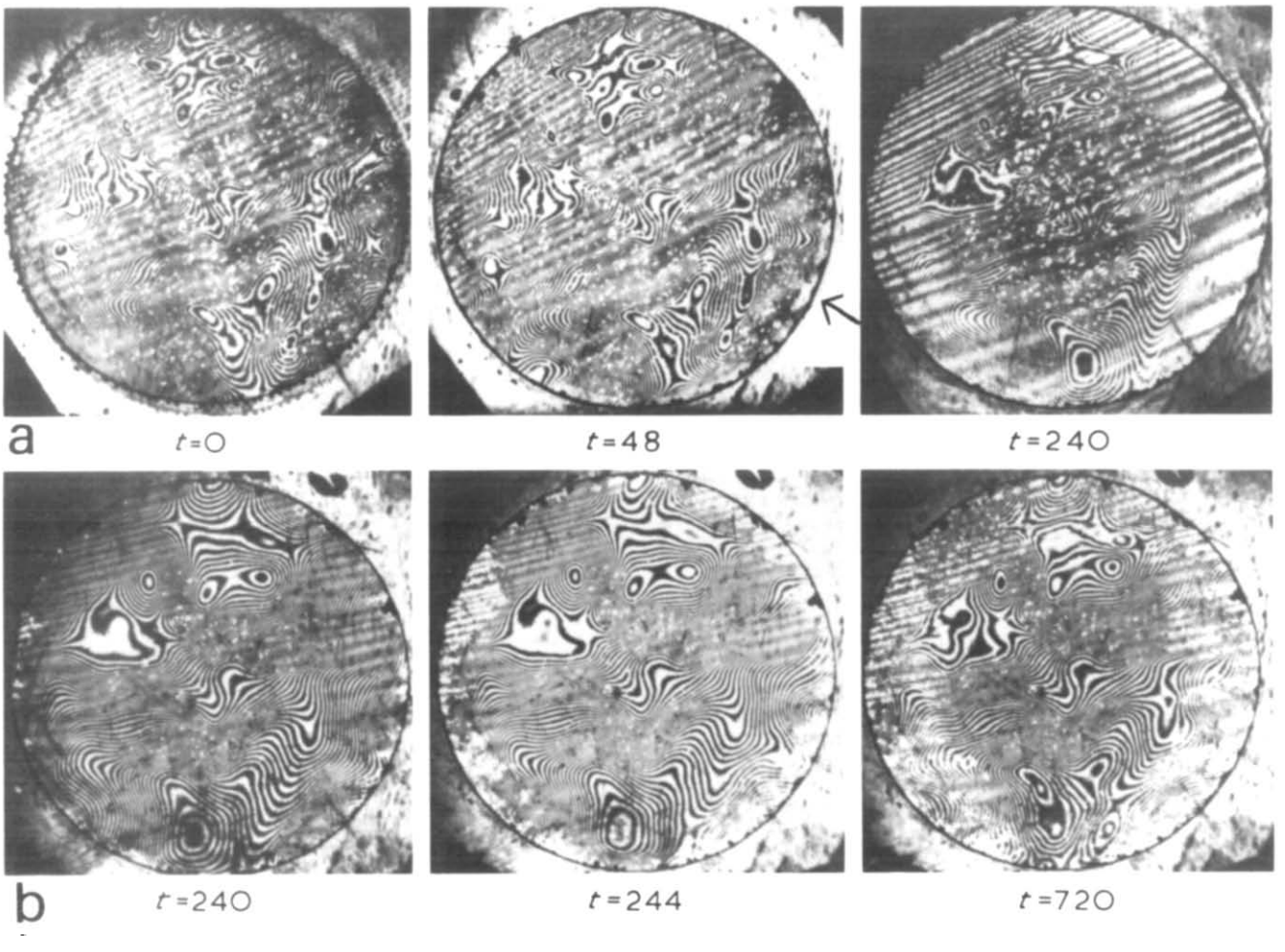

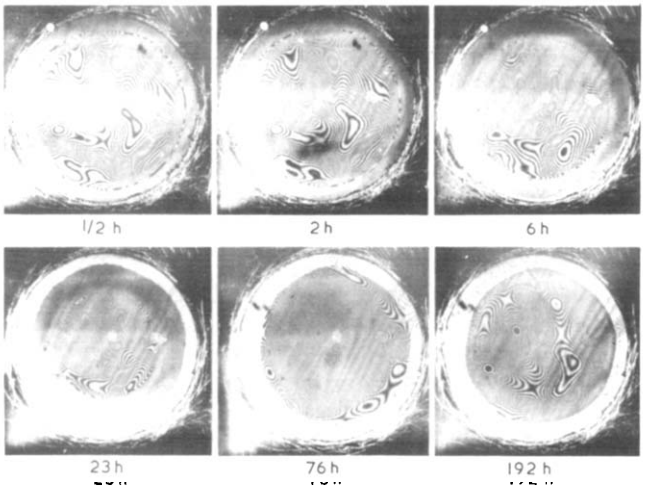

Figure 5 Sequence of interference photographs for a FM 1000 specimen immersed in distilled water at 81°C

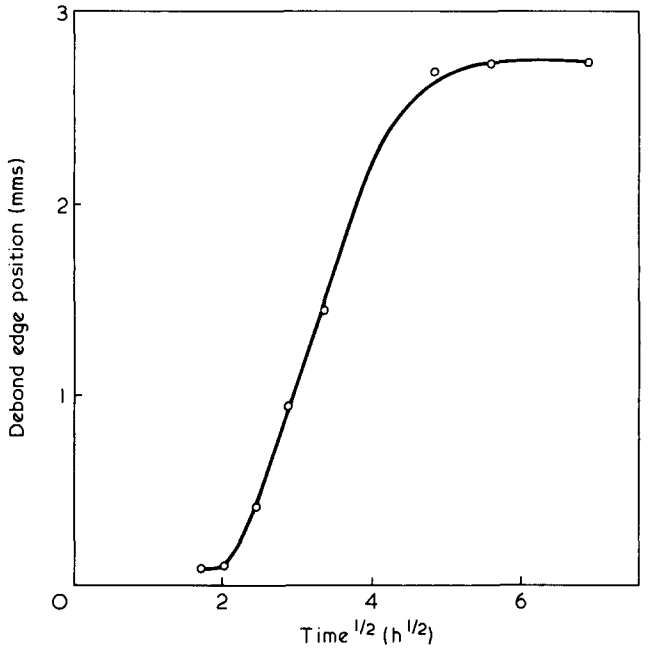

Figure 6 Graph of the position of the debonding edge at the cover slip/adhesive interface plotted as a function of time$^{1/2}$ for the specimen shown in *Figure 5*

sandwiched between a rigid titanium substrate and a cover slip; distilled water immersion was carried out at 81°C. A graph of the position of the debonding edge at the adhesive/cover slip interface, plotted against the square root of time is shown in *Figure 6*.

FM 1000 is characterized by a particularly large hygro coefficient of expansion[3] and *Figure 7* shows the swelling behaviour for a joint manufactured from this material. To maintain contact with the outer annulus of swollen resin (*Figure 7(c)*), the adherends would each need to bend with curvature that is opposite to that inside the boundary between swollen and unswollen adhesive. Failure to adopt such 'S' wise bending manifests itself as the observed circumferential crack.

If it is assumed that the rate of debonding is linearly related to the swelling kinetics (this may or may not be valid in view of the complicated 'opposite curvatures' elastic deformation of the cover slip) and that the swelling kinetics are described by simple diffusion equations, then it should be possible to use measurements of debonding rates in order to estimate the water concentration at which debonding occurs. Kinloch[4] has written and successfully used a computer program for just this purpose, and measurements from *Figure 5* have been processed by Kinloch[5] and predict the critical water concentrations shown in *Figure 8*. It should be pointed out that in this computation the diffusion distance is measured from the edge of the joint and not from the debonding edge.

Conclusions

Measurements of dimensional changes produced when a butt joint consisting of a microscope cover slip/FM 73M adhesive film/rigid substrate is subjected to alternate periods of immersion in distilled water and exposure to dry air, both at 62°C, demonstrate that reversible changes occur when the period of water immersion is less than 1 day, but that irreversible changes take place after longer times.

Measurements on a joint consisting of a microscope cover slip/FM 1000 adhesive film/titanium substrate and immersed in water at 81°C leads to easily resolved circumferential debonding.

Acknowledgements

The authors gratefully acknowledge support from the Science Research Council (Grant No. GR/A/8261-1), from the US Air Force (Grant No. AFOSR-77-3448B)

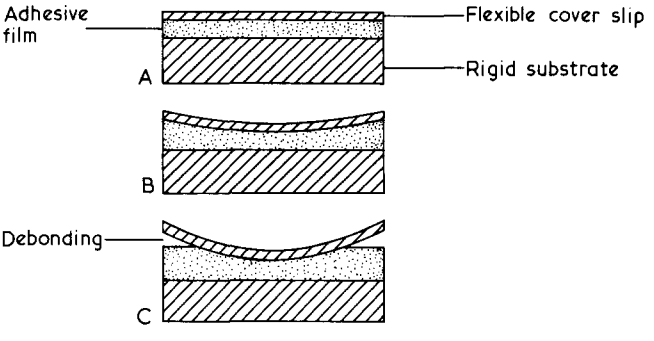

Figure 7 Schematic diagram to illustrate the changing geometry of the cover slip during swelling of the adhesive in a joint exposed to an aqueous environment. Debonding follows saturation of swelling at the rim of the joint

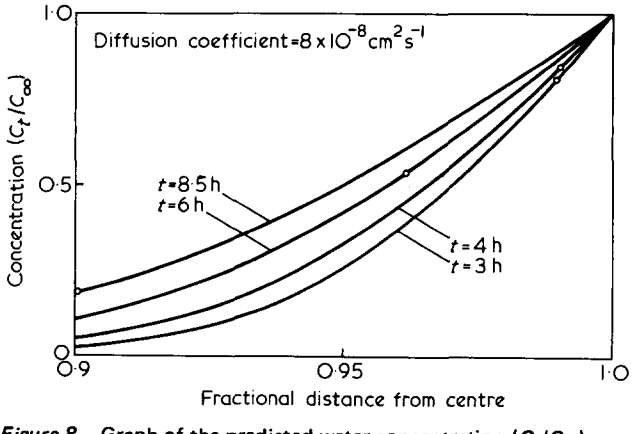

Figure 8 Graph of the predicted water concentration (C_t/C_∞) as a function of fractional distance from the centre of the specimen. ○, points representing the critical concentrations for positions corresponding to the debonding edge shown in *Figure 6*. After Kinloch[5]

and from the US Army (Grant No. DA-ERO-78-G-117). They would also like to thank Dr A. J. Kinloch (Ministry of Defence, PERME) for helpful correspondence and N. L. Bottrell of Westland Helicopters Ltd. for supplying some of the materials.

References

1 Sargent, J. P. and Ashbee, K. H. G. *J. Adhesion* 1980, **11**, 175–189
2 Halpin, J. Cambridge short course on 'Designing with Fibrous Composites', August 1980
3 Sargent, J. P. and Ashbee, K. H. G. *Polymer Composites* 1980, **1**, 93–97
4 Gledhill, R. A., Kinloch, A. J. and Shaw, S. J. *J. Adhesion* 1980, **11**, 3–15
5 Kinloch, A. J. private communication

First results of small and wide angle X-ray scattering of poly(ethylene oxide)/poly(methyl methacrylate) binary blends

Ezio Martuscelli
Istituto di Ricerche su Tecnologia dei Polimeri e Reologia del C.N.R. Arco Felice, Napoli, Italy

and M. Canetti, L. Vicini and A. Seves
Stazione Sperimentale Cellulosa Carta e Fibre Tessili, Milano, Italy
(*Received* 3 *August* 1981; *revised* 6 *November* 1981)

Some preliminary small and wide angle X-ray scattering results are reported from isothermally crystallized samples of poly(ethylene oxide)/(methyl methacrylate) binary blends.

Keywords Analysis; X-rays; X-ray scattering; poly(ethylene oxide); poly(methyl methacrylate); blends; crystallization

Introduction

The crystallization and the thermal behaviour of thin films of poly(ethylene oxide)/poly(methyl methacrylate) (PEO/PMMA) blends obtained by solution casting from chloroform, was investigated by Martuscelli and Demme in a previous work[1]. The results of this study may be summarized as follows:

(i) The dilution of PEO with PMMA causes a depression of the sperulite growth rate. This depression is greater the larger the concentration of non-crystallizing component and the lower the crystallization temperature is.

(ii) The examination, by optical microscopy, of isothermally crystallized thin films of PEO/PMMA blends shows that down to 70% PEO the sample is completely filled with spherulites and no segregation phenomenon of the amorphous component is observed.

(iii) At the same crystallization temperature the observed melting temperature (T_m) of PEO/PMMA blends is lower than that of pure PEO. This effect is more pronounced at lower T_c whilst it is almost negligible at low undercooling.

(iv) For blend samples and for high values of undercooling, T_m increases linearly with T_c. At a well defined value of T_c an abrupt change in the slope is observed. The trend is no longer linear and for lower undercooling the melting point depression tends to disappear.

These observations, together with the finding that in the case of PEO/PMMA blends with high PMMA content the glass transition temperature decreases with increasing PEO content, led the authors to the conclusion that PEO and PMMA are compatible in the melt even if the thermal behaviour of such blends suggests a lower critical solution temperature behaviour below the melting temperature of PEO.

In this communication we report on some preliminary results concerning the analysis of the small and wide angle X-ray scattering of isothermally crystallized samples of PEO/PMMA blends. The main goal of this work is to gain more information about the structure and the overall morphology of such blends by finding some correlation between long spacing, crystal size, composition and crystallization conditions.

Experimental

The characteristics and the source of the polymers are reported in *Table 1*. Films of PEO/PMMA blends were prepared by solution casting from chloroform on glass plates placed on a hot plate set at 50°C. To ensure removal of the solvent the films were kept under vacuum at 70°C for 24 h.

The following compositions were investigated: PEO/PMMA (90/10), (80/20) and (70/30) (w/w).

Table 1 Characteristics of PEO and PMMA

	PEO	PMMA
Source	Fluka AG	BDH
Molecular weight	20000	116000[a]
Melting temperature	65°C	–
Glass transition temperature	−60°C	100°–110°C
Melt flow index (10 Kg)	–	1.0
Melt viscosity 240°C (Shear rate 1120 s^{-1})	–	3.25 K poise

[a] Average viscosity (in chloroform at 25°C)

0032-3861/82/030331-04$03.00
©1982 Butterworth & Co (Publishers) Ltd.